Journal of Applied Polymer Science

Effect of *in situ* apatite on performance of collagen fiber film for food packaging applications

Wenhang Wang,[1,2] Yaowei Liu,[1,2] Anjun Liu ,[1,2] Yana Zhao,[1,2] Xin Chen[1,2]

[1]Key Laboratory of Food Nutrition and Safety, Ministry of Education, College of Food Engineering and Biotechnology, Tianjin University of Science and Technology, Tianjin 300457, China

[2]Tianjin Food Safety & Low Carbon Manufacturing Collaborative Innovation Center, 300457, Tianjin, China

Correspondence to: W. Wang (E-mail: wangwenhang@tust.edu.cn or Laj@tust.edu.cn)

ABSTRACT: This study attempted to prepare apatite *in situ* in acid-swollen cowhide collagen film by an ammonia gas fumigating method and assess its reinforcement effect on a collagen fiber film for food packaging applications. The X-ray diffraction and Fourier transform infrared spectroscopy results confirmed the successful synthesis of apatite in collagen fiber films. SEM images showed that tiny apatite particles appeared as a coating on the film surface and also made the film's inner structure more compact and less porous than pure collagen fiber film. Apatite significantly ($p < 0.05$) increased the tensile strength and improved the water vapor barrier and water insolubility properties of collagen fiber film. Moreover, the thermogravimetric and differential scanning calorimetry results confirmed that the thermal stability of collagen was improved with the increasing apatite. The *in situ*–synthesized apatite provided a practical reinforcement approach to improving the collagen fiber film's performance and benefited its application as a food packaging material. © 2016 Wiley Periodicals, Inc. J. Appl. Polym. Sci. **2016**, *133*, 44154.

KEYWORDS: films; packaging; proteins

Received 9 April 2016; accepted 4 July 2016

DOI: 10.1002/app.44154

INTRODUCTION

Biodegradable and edible films have been mainly obtained from biopolymers,[1] such as protein, polysaccharide, lipid, and their combinations.[2] Among them, protein and protein-based films are of great value and have good prospects because of their nutritional value and film-forming characteristics, good barrier property, superior mechanical property, and so on.[3] Some proteins, such as whey protein,[2] peanut protein,[4] and gelatin,[5] have been studied widely in recent years. In addition, collagen, the most abundant protein in animals, has been applied as an important material in medical and bioengineering applications because of its biodegradability, weak antigenicity, and so on.[6] Moreover, the unique triple helix structure endows collagen with superior mechanical strength.[7] In food applications, collagen has long been successfully used as an artificial casing preparation.[8] Physiologically, four to eight collagen molecules aggregate via fibrillogenesis into microfibrils.[9] With further self- aggregation and intermolecular crosslinks, these microfibrils further change into collagen fibrils with diameters ranging from 10 nm to 500 nm, which have extra strength and stability.[7] These fibrils further overlap to form collagen fibers, which possess a high degree of axial alignment of collagen molecules and are characterized by a regular stagger of approximately one-quarter of a rod length between each molecule and its axially aligned neighbor.[10] Collagen fiber, commonly obtained from animal skin, such as bovine hide and pig skin,[11] has an internal axis with large numbers of thin filaments that endow the collagen fibers with elasticity and a strong mechanical property via self-aggregation and crosslinking.[9] Because of its super strength, collagen-based artificial casing was successfully commercialized in the 1980s. Recently, with the development of edible and biodegradable packaging in food processing, collagen films are regaining increasing interest in the food field, with a few research studies on scientific evaluation,[12] technological design,[13] and efficient enhancement[14] of film performance. Although collagen film shows a strength superior to other protein films, it still needs to be treated to obtain further performance. Some attempts have been recently made in the food-related areas. Wang *et al.*[8] reported that ultraviolet irradiation (UV) and dehydrothermal treatment (DHT) could be potentially used as safe alternatives to chemical crosslinking for the production of collagen casing. Moreover, collagen can be combined with some heterogeneous fillers, such as chitosan,[15] which could improve the safety, quality, and health benefits of sausages because of its innate antioxidant properties. Additionally, some cogelling proteins,

such as blood plasma protein, soy protein isolate, whey protein isolate, and gluten, provided a suitable approach to modifying collagen film strength.[2]

Hydroxyapatite (HA), an inorganic substance, accounting for 69–80 wt % of bone weight,[16,17] in fact has a stoichiometrically deficient amount of hydroxyl, which was replaced by carbonate ion or other ions.[18] The substitutions provide the biomineral with a variety of names, such as apatite, hydroxyapatite, carbonated hydroxyapatite, and so on in the literature; it will be referred to simply as apatite in this study. Because of its distinct material character, such as naturally existing in bone,[19] apatite works well with collagen in biology-related fields[20,21] and is now widely applied as a substitute material for some bioengineering fields, such as filling bony defects.[17] Besides, given its superior bioactivity, osteoconductivity, biocompatibility, nontoxicity, and osseointegration, many investigations have focused on using HA as filler to reinforce some natural polymers like alginate, gelatin, chitosan, and collagen and produce high-quality composites.[22–24] Among them, collagen–HA composite materials have aroused significant attention and have good prospects since they have excellent biocompatibility and bioactivity, as well as improved mechanical properties. For example, a new material with collagen and hydroxyapatite was prepared to simulate some good properties of natural bone, presenting some expected results.[20,21] Moreover, Goes *et al.*[17] studied the different effects of apatite formed by an alternate soaking process on anionic collagen and native collagen films.

For the addition of HA, both *in situ* and *ex situ* processes have been used. *Ex situ* refers to hydroxyapatite that is first prepared and then simply mixed into the biopolymers.[24] Thus, the hydroxyapatite might not solidly adhere to the biopolymers and are delivered from the matrix, therefore reducing the designed functionality of HA. In order to enhance the interaction between the inorganic apatite and the organic polymers, plenty of people have made many trials. Among them, coatings[25,26] and *in situ* synthesis[17,27] were most studied. According to Goes *et al.*,[17] apatite was formed by a process of alternately soaking in a 200 m*M* $CaCl_2$ solution and a 200 m*M* K_2HPO_4 solution. Further, it was reported that hydrophilic polar groups such as phosphate[28] and carboxyl and hydroxyl groups were beneficial to the interaction between apatite and the collagen polymers.[29] Organic polymers containing carboxyl groups could form apatite on their surfaces in the presence of calcium ions since the carboxyl groups induce apatite nucleation and the calcium ions accelerate apatite nucleation.[30,31]

In this study, a novel *in situ* fabrication of apatite was attempted using an ammonia gas fumigating method, and its reinforcement effect on collage fiber films was investigated. First, acid-swollen collagen fibers were prepared from cowhides as a basic film-forming material in a diluted hydrochloric acid solution. The high-viscosity collagen syrup was mixed with disodium hydrogen phosphate and calcium chloride homogeneously, and then the mixture was cast and fumigated in ammonia gas to produce apatite, followed by drying to form films. The graphical processing technology of *in situ* fabrication of apatite and the apatite-containing collagen fiber film was as shown in Figure 1. X-ray diffraction (XRD) and Fourier transform infrared spectroscopy (FTIR) were applied to confirm the presence of apatite and study the effects of apatite on the conformation changes of collagen molecules. Furthermore, the effects of apatite on the collagen fiber film's packaging-related properties, including mechanical character, water vapor barrier property, solubility in water, thermodynamic stability, and microstructures, were investigated.

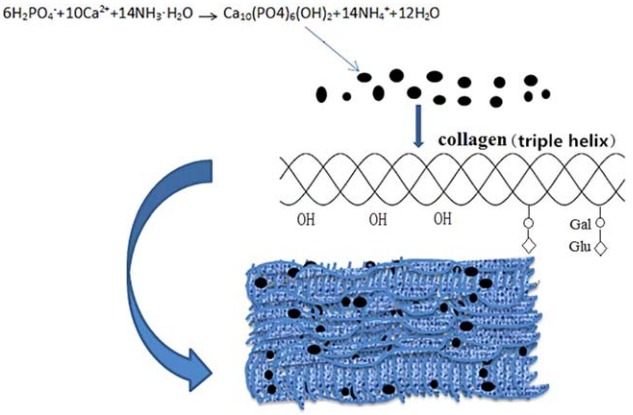

Figure 1. Graphical illustration for the *in situ* synthesis of apatite and the resulting formation of apatite-reinforced collagen fiber film derived from acid-swollen cowhide. [Color figure can be viewed in the online issue, which is available at wileyonlinelibrary.com.]

EXPERIMENTAL

Chemicals

Limed cowhide was kindly offered by a local leather processing plant in Hebei, China. Disodium hydrogen phosphate, calcium chloride, glycerin, and hydrochloric acid were purchased from Sigma-Aldrich (Shanghai, China). All other chemicals were all analytical grade and used without further purification.

Collagen Fiber and Film Preparation

Collagen fibers were prepared by the acid-swelling method[14] with a little modification. Briefly, limed cowhide was cut into pieces (5 cm × 5 cm) and washed by several portions of distilled water until the pH approached 7.0. Then, the pieces were immersed in a 0.02 *M* hydrochloric acid solution at a ratio of 1:3 (cowhide to acid solution, m/v) at 25 °C for 36 h to swell completely. After that, the swollen cowhides were shredded and ground to obtain a homogeneous fine collagen syrup. In order not to make denaturated collagen, the whole process should be conducted below 25 °C.

Films were prepared by casting and dehydration of 40 mL collagen syrup (containing 0.6 g dry collagen fiber) with a certain amount of glycerol (30 g per 100 g of collagen fiber) as plasticizer according to the methods proposed before[5,13] with minor modifications. Briefly, a predetermined amount of collagen syrup and glycerol were mixed to form a basic film-forming paste. Then, according to eq. (1), a series of appropriate proportions of sodium dihydrogen phosphate and calcium chloride were added into the paste to reach the final apatite concentrations of 0, 0.42, 0.83, 1.25, and 1.67 mmol/g. After stirring for 30 min, the mixtures formed into colloidal dispersions and were poured

onto 12 cm × 12 cm Plexiglas plates and dried at 25 °C for 12 h. After that, the Plexiglas plates covered with semidry films were moved into a hermetic box equipped with 5 *M* ammolonium hydroxide to neutralize them until the pH reached about 7.0, wherein the apatite was formed. After that, they were rinsed five times in distilled water to remove the redundant ions, followed by dehydration in an oven at 30 °C for 6 h with good ventilation. The prepared films were conditioned in desiccators at 51% relative humidity (RH) with a saturated magnesium nitrate solution for 5 days at 25 °C.[5]

$$6H_2PO_4^- + 10Ca^{2+} + 14NH_3 \cdot H_2O = Ca_{10}(PO_4)_6(OH)_2 + 14NH_4^+ + 12H_2O \quad (1)$$

Gel Electrophoresis

The protein patterns of the collagen fibers were analyzed via one-dimensional sodium dodecyl sulfate–polyacrylamide gel electrophoresis (1D SDS-PAGE) using an 8% separation gel and 5% stacking gel according to the previous method by Skierka.[32] Collagen samples were dissolved in a sample buffer (Tris-HCl, pH 6.8, containing 2-mercaptoethanol, 4% SDS). Samples containing approximately 2 μg of collagen/μL were heated at 100 °C for 5 min. Samples of 20 μL were loaded per well, and protein bands were stained with Coomassine Brilliant Blue R250. High-molecular-weight markers (Sigma Chemical, St. Louis, MO) were used to estimate the molecular weights of the proteins. 1D SDS-PAGE was performed at a constant voltage of 120 V on a miniVE apparatus (Bio-Rad, Hercules, California, USA), and the image of the gel was captured using an image scanner (Bio-Rad).

Particle Size Measurements

Collagen particle sizes were measured in a BT-90 dynamic light scattering nanometer laser granulometer (Bettersize Co., Dandong, Liaoning, China) with a scattering angle of 90° and a light source (He-Ne laser) of fixed wavelength of 635 nm. First, 25 mg of collagen was dissolved in 5 mL acetic acid solution (pH = 2.0) to prepare the collagen solution. Then, 5 mL of collagen solution was poured into a cuvette and measured using the dynamic light scattering method.[33]

Attenuated Total Reflectance FTIR

Attenuated total reflectance (ATR) FTIR spectra of the collagen fiber–apatite composite film, hydroxyapatite, and pure collagen fiber film were characterized using a Thermo Nicolet Avatar 370 FTIR spectrometer (Thermo, Shanghai, China). Each sample was subjected to 32 scans per sample at 4 cm^{-1} resolution from 4000 to 500 cm^{-1}.[5]

X-ray Diffraction

The XRD patterns were obtained using a Lab-X XRD-6100 diffractometer (Shimadzu, Tokyo, Japan). Film samples of 3.3 cm × 3.5 cm were fixed on the platform and stuck in the circular clamp of the instrument. The parameters were set as follows: voltage and current: 40 kV and 30 mA, respectively; scan range: 2θ, from 5° to 65°; step: 0.1°; and speed 2°/min.

Film Thickness

A digital micrometer (Mitutoyo No. 293-766, Tokyo, Japan) with a precision of 0.001 mm was used to measure the thickness of the films. The thickness value reported was the mean of 10 random measurements.

Opacity and Color Parameter

The opacity of the films was determined with the method described previously. In brief, films were cut into pieces 4 cm × 1 cm and adhered to one side of a quartz colorimetric utensil, and the light absorbance at a wavelength of 600 nm was recorded using a Genesys 10s UV-VIS spectrophotometer (Thermo Scientific, Waltham, Massachusetts) with air as reference. The opacity of the films was expressed as absorbance units per thickness unit, and each sample was tested in triplicate.

The surface color of the collagen fiber–apatite composite films was analyzed with a colorimeter (CR-700d Minolta Chroma Meter; Konica Minolta Sensing Inc., Tokyo, Japan) according to the method proposed before.[4,34]

Mechanical Properties

The tensile strength (TS, MPa) and percentage of elongation at break (EL, %) of the composite films were determined using a Texture Analyzer (Stable Micro Systems Ltd., Surrey, London, UK), with an initial grip separation of 30 mm and a test speed of 2 mm/s.[5,35] In short, the films were cut into rectangular test strips with a width of 25 mm and length of 70 mm with a metal scissors. The maximum tensile strength and elongation at break were recorded. The film TS was calculated by dividing the maximum load at break by the area of the cross section and expressed in MPa. Film elongation (%EL) was expressed as follows:

$$\%EL = (L_1 - L_0)/L_0 \times 100 \quad (2)$$

where L_0 (mm) was the initial length of the film and L_0 (mm) was its length at break.

Water Vapor Permeability and Solubility in Water

The water vapor permeability (WVP) of the collagen fiber–apatite films was measured using a method reported in the literature.[36,37] The composite films were cut into pieces 4 cm in diameter, and the film was used to seal a testing cup containing anhydrous calcium chloride. The films were allowed to equilibrate for 1 h before the cells were initially weighed. Thereafter, the weight of the cup was measured intermittently at intervals of 24 h, up to 96 h. The WVP of the films was calculated as follows:

$$WVP = W \times L/A \times T \times P \quad (3)$$

where WVP indicates the water vapor permeability ($\times 10^{-11}$ g m/Pa m^2 s), and *W, L, T, A*, and *P* indicate the increased cup weight (g), thickness of the film (m), measuring time (s), measuring area (m^2), and difference in pressure between outside the cup and inside the cup (Pa), respectively.

The solubility in water for the collagen fiber–apatite films was determined as described previously[4,35] with some modifications. In short, randomly selected samples cut from each film were dried in an oven at 105 °C until achieving constant weight. The initial dry weight of the samples was recorded. After that, the samples were immersed in the test beakers with 20 mL of distilled water and were placed at room temperature with periodic gentle agitation for 24 h. The insoluble films were removed and dried again in an oven at 105 °C until they reached a constant weight. The solubility (%) of the samples was calculated as follows:

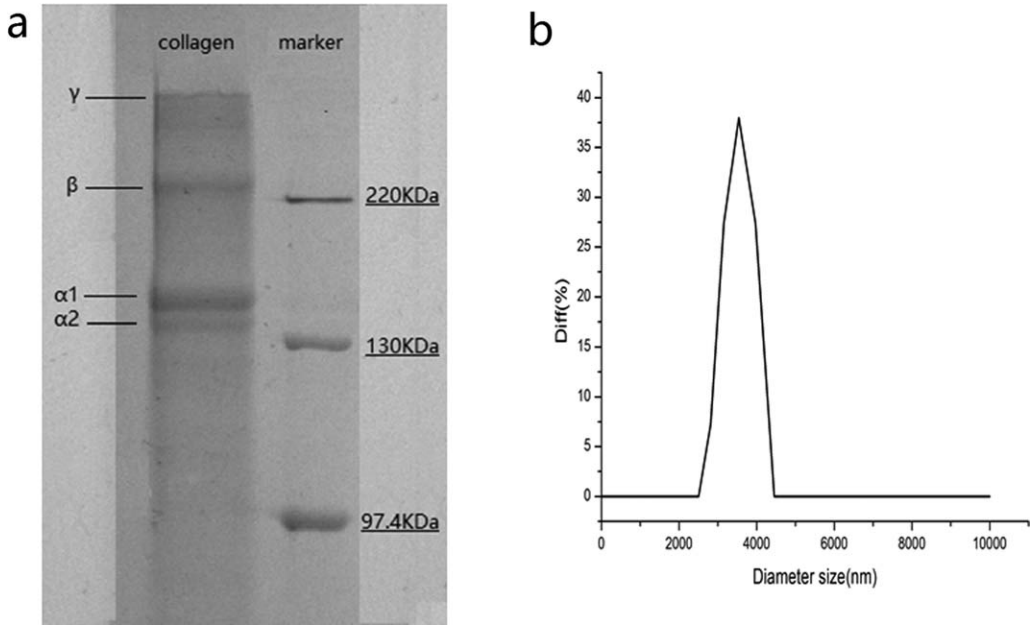

Figure 2. Protein patterns (a) and particle size distribution (b) of collagen fibers.

$$\text{Solubility } (\%) = (w_1 - w_2) \times 100 / w_1 \quad (4)$$

where w_1 (g) was the initial dry weight and w_1 (g) was the final dry weight.

Differential Scanning Calorimetry and Thermogravimetric Analysis

The thermal properties of the collagen fiber–apatite composite films were characterized with a differential scanning calorimeter (DSC) TA-60WS (Shimadzu) according to the published literature[38] with minor modifications. Prior to measurement, the samples were conditioned at 25 °C and 0% RH for 1 week in a desiccator, and ~4 mg of film was sampled and placed in the DSC crucibles (Shimadzu). The samples were heated from 25 °C to 200 °C at a heating speed of 10 °C/min.

Further, dehydrated films were scanned using a thermogravimetric analyzer (Q50 TGA, TA, New Castle, Delaware) from 25 to 600 °C at a rate of 10 °C/min.[39] Nitrogen was used as the purge gas at a flow rate of 40 mL/min.

Scanning Electron Microscopy

The microstructures of the composite films were observed using a scanning electron microscope (SEM; SU1510, Hitachi, Tokyo, Japan) following the method in the literature.[5,36] In order to prepare good cross sections, the films were frozen in liquid nitrogen and cryofractured. Prior to scanning, the samples were fixed to the stage with double-sided adhesive tape and sprayed with a layer of gold in a vacuum room. Then samples were transferred to the cold stage of the SEM chamber and observed at an acceleration voltage of 20 kV and a magnification of 2000×.

Statistical Analysis

All data were expressed as the mean ± standard deviation (SD). Analysis of variance (ANOVA) was used for analysis of the test results (least significant difference) at the significance level of p-value < 0.05 using SPSS 18.0 statistical software (SPSS, Chicago, IL).

RESULTS AND DISCUSSION

SDS-PAGE Pattern of Collagen

Electrophoretic patterns of the prepared collagen are illustrated in Figure 2(a). Compared to the protein markers, the four clear bands of collagen samples showed molecular weights of 354.36 KDa, 251.05 KDa, 163.17 KDa, and 151.47 KDa using the software Quantity One (Bio-Rad). These bands can be identified as gamma (γ), beta (β), alpha 1 (α1), and alpha 2 (α2), indicating it belongs to the classical type I collagen, based on the analysis of ovine tendon collagen.[40]

Collagen Size Distribution

Particle size measurements using dynamic light scattering were performed to determine the hydrodynamic size of the collagen fibers. As shown in Figure 2(b), the size of the collagen fibers ranged from about 3 to 4 μm, with distributions of 2811–3154 nm, 3154–3539 nm, 3539–3971 nm, and 3971–4456 nm as 7.22%, 27.42%, 37.97%, and 27.39% of the total bulk, respectively. Additionally, the volume-weighted mean (D4,3) and the surface-weighted mean (D3,2) particle diameter of the hydrodynamic size of the collagen fibers was calculated to be 3575 nm and 3530 nm, respectively.

FTIR Analysis

The FTIR spectra of hydroxyapatite, pure collagen fiber film, and the composite film with 1.67 mmol/g apatite are illustrated in Figure 3. In the pure collagen fiber film, an amide-A band (N—H) was observed at the wavenumber of ~3320 cm^{-1}.[39] The amide-I band (C═O stretching/hydrogen bonding coupled with COO) was noticeable at wavenumber 1657 cm^{-1}, and the amide-I region is probably the most useful for infrared spectroscopic analysis for the second structure of proteins.[41] The amide-II band (bending vibrations of N—H and stretching

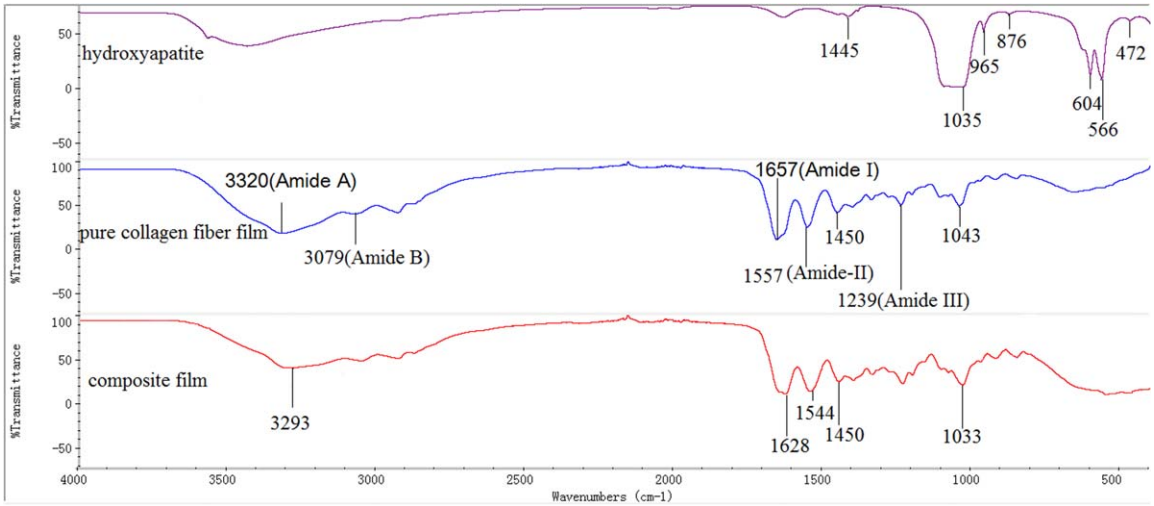

Figure 3. Fourier transform infrared spectra of hydroxyapatite and collagen fiber films. [Color figure can be viewed in the online issue, which is available at wileyonlinelibrary.com.]

vibrations of C—N groups) and amide-III band (vibrations of in-plane C—N and N—H groups of bound amide or vibrations of CH_2 groups of glycine) were observed at wavenumbers 1557 cm^{-1} and 1248 cm^{-1}, respectively.

For HA, resonances associated with the stretching mode of the $(PO4)^{3-}$ ion were observed at 1035 and 965 cm^{-1}. Resonances associated with the stretching mode of the $(CO_3)^{2-}$ ion were also observed at 876 cm^{-1}. The peaks at 566 and 604 cm^{-1} belong to the vibrations (υ_4) of the phosphate group of HA. The resonances around 1445 cm^{-1} are the result of carbonate stretching vibrations.[27]

For the composite film, it was noted that the amplitudes of amide-A, amide-I, and amide-II in the composite film decreased obviously compared with the control film. This might be due to the higher protein content in the pure collagen fiber film, which could prevent the absorption of HA.[39] Meanwhile, the wavenumbers of the amide-A, amide-I, and amide-II peaks shifted to 3293 cm^{-1}, 1628 cm^{-1}, and 1544 cm^{-1}, respectively, while amide-B and amide-III did not have great differences. All these changes can likely be attributed to the presence of apatite. According to the study by Zhai and Cui,[22] amide-I (C═O bands) should be the nucleation sites of calcium phosphate, which present a red shift and weaken in amplitude once forming calcium phosphate on collagen. Furthermore, the peak at ~1450 cm^{-1} is related to pyrrolidine ring vibrations, which suggests that the integrity of the collagen structure was maintained.[17] Additionally, the typical absorption peaks of HA were not observed in the composite film, presumably due to its lower concentration.

X-ray Diffraction

Figure 4 presents the X-ray diffraction patterns of apatite, pure collagen fiber film, and the collagen fiber–apatite composite film (apatite concentration 1.67 mmol/g). For the collagen film, a broad band was observed at 20°, suggesting the low crystallinity of collagen molecules. For the composite film, a high degree of crystallization was observed, and it is quite similar to that of hydroxyapatite. This is potentially attributed to the presence of abundant apatite crystals in the film matrix. In the collagen–HA composite film, we can notice the presence of other peaks that do not belong to the HA phase. This is an indication of the formation of other crystalline phases of apatite.[27] In addition, for the composite film, two peaks at around 26° and 32° were observed, and, according to Goes *et al.*,[17] these are assigned to the main peaks for the apatite crystals. These results suggest that certain kinds of apatites were synthesized in our study, and they modified the crystallinity of the collagen fiber film to a great extent.

Thickness, Opacity, and Color Properties of the Films

The thickness, opacity, and color parameters of the collagen fiber–apatite composite film are presented in Table I. It seems that the presence of apatite did not exert a significant influence on the film thickness but has an obvious impact on film color and transparency. The values of L^* and b^* were both increased

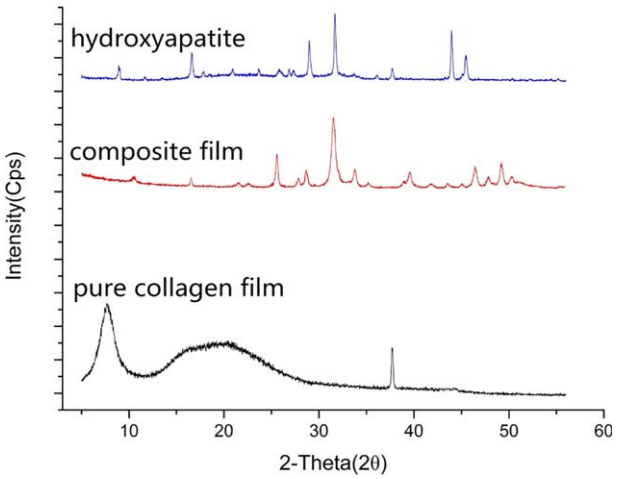

Figure 4. X-ray diffraction patterns of hydroxyapatite and collagen fiber films. [Color figure can be viewed in the online issue, which is available at wileyonlinelibrary.com.]

Table I. Thickness, Opacity, and Color Parameters of Collagen Fiber–Apatite Composite Films ($n \geq 3$)

Apatite content per 1 g collagen (mmol/g)	Thickness (μm)	L^*	a^*	b^*	Opacity
0	78.0 ± 7.62	85.47 ± 0.13^a	-0.73 ± 0.02^a	-3.00 ± 0.05^a	0.15 ± 0.02^a
0.42	73.5 ± 10.07	86.97 ± 0.12^b	-0.67 ± 0.01^a	-2.10 ± 0.06^b	0.17 ± 0.02^a
0.83	71.8 ± 7.96	87.44 ± 0.17^c	-0.66 ± 0.12^a	-1.23 ± 0.11^c	0.22 ± 0.01^b
1.25	73.5 ± 11.84	87.48 ± 0.11^d	-0.44 ± 0.07^b	0.34 ± 0.08^d	0.26 ± 0.02^c
1.67	71.8 ± 11.18	88.01 ± 0.19^e	1.38 ± 0.16^c	2.49 ± 0.24^e	0.42 ± 0.01^d

a to e: Means within the same graph that show different letters indicate significantly different ($P < 0.05$).

significantly with the increasing apatite amount ($p < 0.05$), indicating that the color intensified as the apatite amount increased. The photographs of the prepared films with different apatite contents are also displayed in Figure 5, presenting an increase in opacity that depended on the amount of HA. These color changes in the film samples are in accord with the color parameters depicted in Table I. In addition, the increased opacity of the collagen fiber film suggests that the inclusion of apatite in the collagen film caused less light to pass through the film. With the growing amount of sodium dihydrogen phosphate and calcium chloride, there would be more apatite, and the particle size would also be larger, facilitating the increased opacity. A similar trend was observed in the preparation of fish gelatin–laponite biohybrid elastic coacervates.[42,43]

Mechanical Properties

The effects of apatite amount on the tensile strength and elongation of collagen fiber–apatite composite films are demonstrated in Figure 6(a,b). As depicted in Figure 6(a), *in situ* apatite at lower concentration (0.42 mmol/g) has no significant influence on the tensile strength. However, at high concentrations (≥0.83 mmol/g), the presence of apatite significantly increased the TS of the collagen fiber film ($p < 0.05$). The tensile strength was increased by 30.34% when the apatite amount reached 1.67 mmol/g compared to the pure collagen fiber film. These findings may suggest that the *in situ* apatite was well dispersed in the polymer matrix and has a good compatibility with collagen, benefiting the improvement of film TS due to its character mentioned above.

According to Chao *et al.*,[24] apatite, with great hardness, can harden the polymers, making it resistant to crushing. As shown in Figure 7(d), pure collagen fiber film had a feature of porosity; however, with the increasing apatite, the structure of the film clearly became compact. Meanwhile, because crosslinks can dissociate under certain conditions,[9] reconstituted forms of collagen such as films, fibers, or sponges may disintegrate or collapse as a result of insufficient strength. But the occurrence of apatite, as supporters in the network, could make the network more stable and stronger. In addition, according to Chao *et al.*,[24] the presence of numerous functional groups of hydroxyls, amines, and carboxyls are beneficial for enhancing the interfacial bonding between HA and polymer. The *in situ* apatite at low concentrations (≤0.83 mmol/g) has no significant effect on the elongation of the collagen fiber film, as displayed in Figure 6(b).

However, high concentrations of apatite have significant influences on the elongation compared with pure collagen fiber film. The elongation of collagen fiber films with apatite at 1.25 mmol/g and 1.67 mmol/g was reduced by 6.52% and 7.78%, respectively. This change may be attributed to the brittleness and stiffness of apatite.[24] On one hand, the presence of apatite makes the collagen fiber film more resistant to crushing; on the other hand, apatite at high concentrations can restrict the collagen fiber film from extending because of its brittleness.

Water Vapor Permeability and Solubility in Water

The WVP and solubility in water of the collagen fiber–apatite film are shown in Figure 8(a,b). As revealed in Figure 8(a), the WVP of the collagen fiber films declined with increasing apatite content. The WVP of the collagen fiber film with 1.67 mmol/g apatite decreased to 2.30×10^{-11} g m/Pa m^2 s compared with that of pure collagen fiber film (3.52×10^{-11} g m/Pa m^2 s).

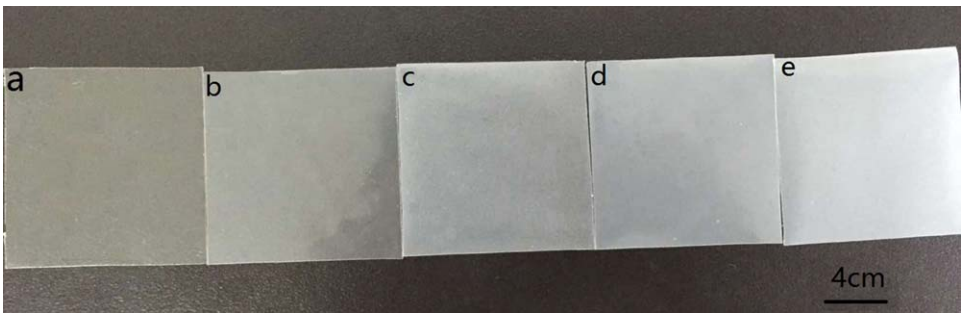

Figure 5. Morphology of prepared films with different apatite contents: (a) 0 mmol/g, (b) 0.42 mmol/g, (c) 0.83 mmol/g, (d) 1.25 mmol/g, (e) 1.67 mmol/g. Pictures of film samples were captured by a digital camera (PowerShot SD 630, Canon, Tokyo, Japan). [Color figure can be viewed in the online issue, which is available at wileyonlinelibrary.com.]

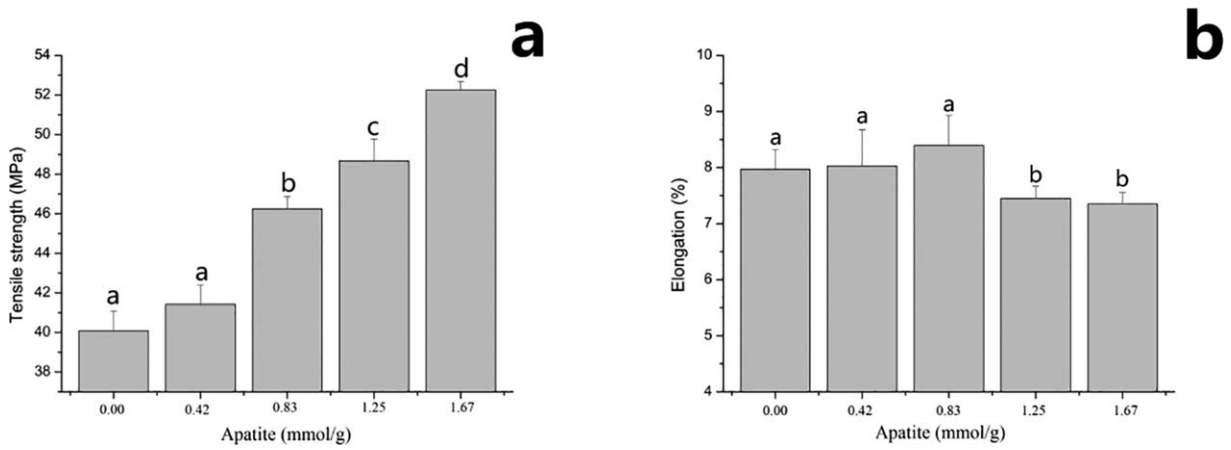

Figure 6. Tensile strength (a) and elongation at break (b) of collagen fiber–apatite composite films. Error bars indicate the standard deviation of three replications. a to d: Means within the same graph that show different letters indicate significantly different ($P < 0.05$).

This result was similar to that of Żenkiewicz and Richert,[44] who observed an obvious reduction in water vapor permeability of polylactic acid–nanoclay films. As displayed in Figure 7, the apatite particles embedded in the collagen network can act as barriers against the movement of water vapor. According to Farahnaky *et al.*[43] and Wang *et al.*,[5] the presence of apatite particles

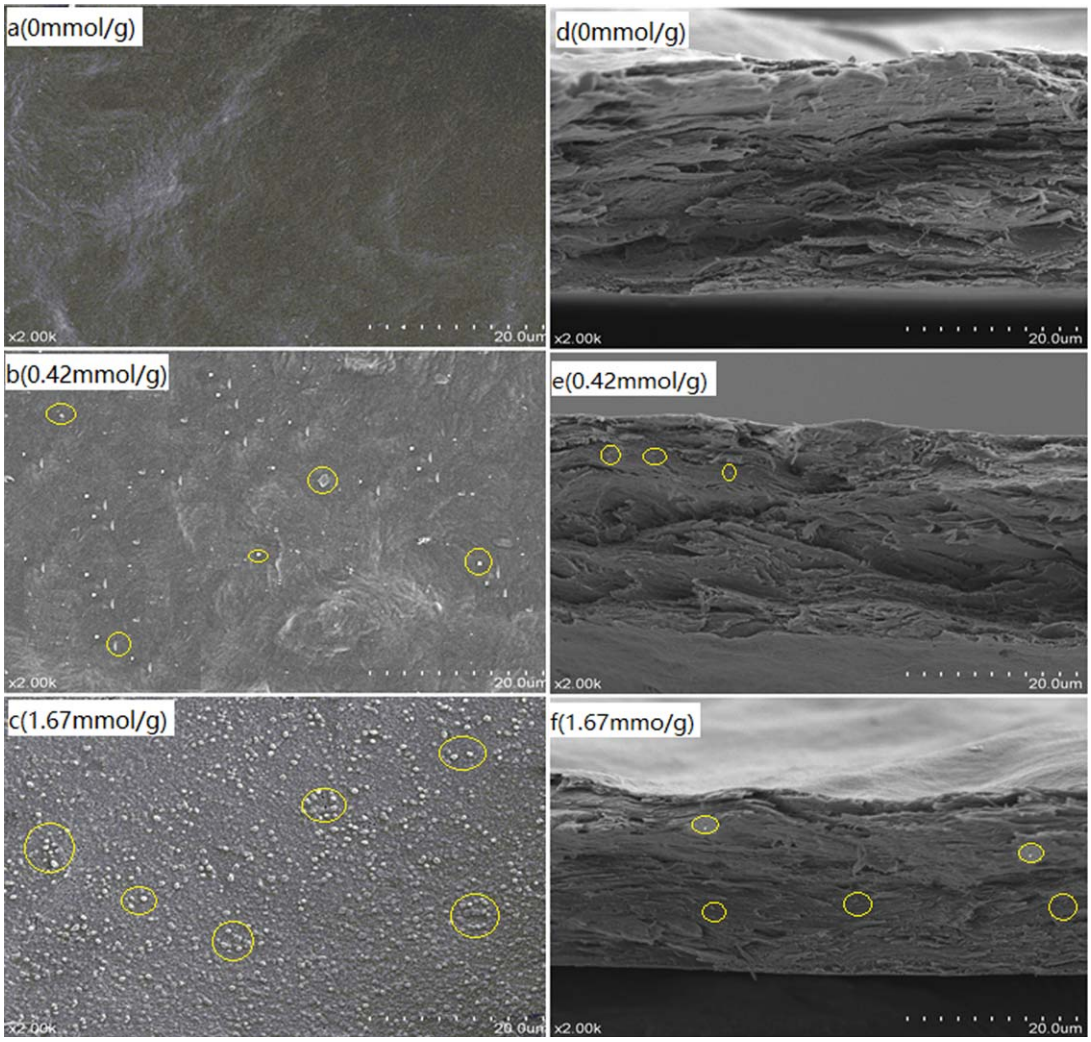

Figure 7. SEM images of surfaces (a–c) and cross sections (d–f) of collagen fiber–apatite composite films. [Color figure can be viewed in the online issue, which is available at wileyonlinelibrary.com.]

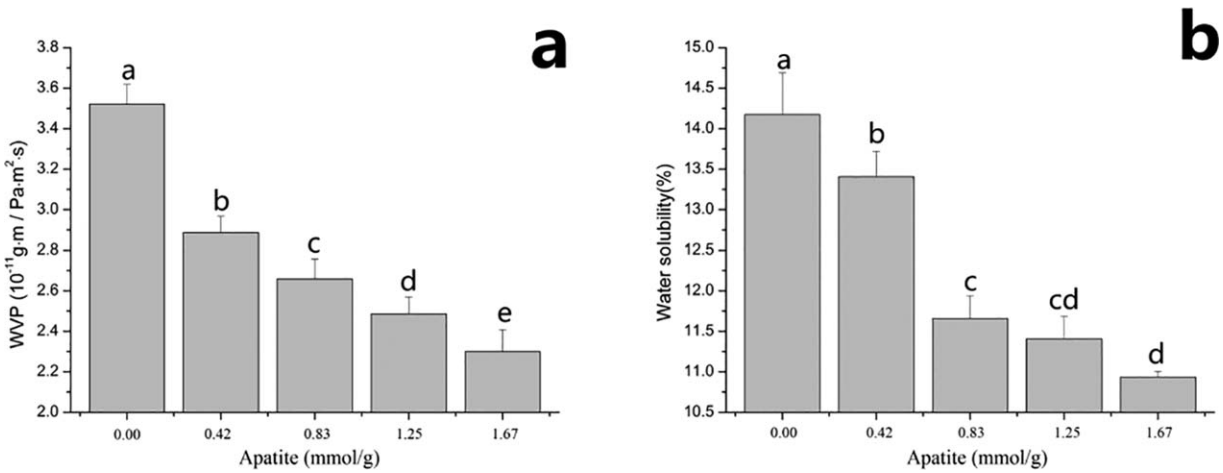

Figure 8. Water vapor permeability (a) and solubility in water (b) of collagen fiber–apatite composite films. Error bars indicate the standard deviation of three replications. a to d: Means within the same graph that show different letters indicate significantly different ($P < 0.05$).

created a more circuitous route in the composite film matrix and also caused the water vapor molecules to travel a longer distance, inducing a low water vapor permeability.

Total soluble matter was determined to measure the solubility of the collagen polymers and apatite particles in an aqueous environment. As shown in Figure 8(b), the water solubility decreased as the apatite concentration rose: the solubility of the collagen fiber–apatite film decreased to 10.93% from 14.17% as the apatite concentration ranged from 0 mmol/g to 1.67 mmol/g. A similar result could be found in the studies of Farahnaky *et al.*,[43] who incorporated clay into a gelatin matrix. This was potentially aroused by the differing hydrophobicity between apatite and collagen fiber. Apatite molecules may aggregate within or over the networks of a collagen fiber film, which could markedly reduce efficient contact between the collagen and water molecules, weakening the hydrophilicity of the collagen polymers.[45]

Thermogravimetric Analysis

The weight loss (TG) curves of collagen fiber films with different amounts of apatite are shown in Figure 9. The degradation temperatures (T_d), weight loss (Δ_w), and residue of all film samples are shown in Table II. All of the samples exhibited three main stages of weight loss. For all films, the first-stage weight loss (Δ_{w1}) at 4.16–7.33% was observed at the temperature (T_{d1}) of 40.92–55.90 °C. This small weight loss is probably due to the loss of free and absorbed water. As shown in the Table II, the lower weight loss in the first stage of composite films compared with the pure collagen fiber film was potentially due to the higher hydrophobicity. The second stage of weight loss ($\Delta_{w2} = 17.02$–25.91%) was observed at the T_{d2} of 202.90–220.31 °C. Glycerol and lower molecular weight protein, such as the small amount of gelatin generated in the process of preparation of the collagen fiber, were likely to degrade at this stage. Hoque *et al.*[46] reported that the degradation temperature for cuttlefish skin gelatin film was 196.30–216.71 °C. For the third stage of weight loss, Δ_{w3} of 40.00–43.10% and T_{d3} of 281.88–290.66 °C were obtained for films incorporated with different contents of apatite. According to Tongnuanchan *et al.*,[39] this was most likely associated with the degradation of the larger size or highly associated collagen fraction.

In general, the three stages of weight loss have some similarity. On one hand, the onset temperature all increased with the apatite concentration in each stage; on the other hand, the weight loss was also almost in reverse proportion to the apatite. In any case, the onset temperature and weight in each stage all declined compared to the pure collagen fiber film. Further, the gradually increased residue was likely to be the epibiotic *in situ* apatite with higher heat resistance or some stable components, and the degradation temperature was not detectable. The results suggested that the film with apatite showed higher heat resistance than the pure collagen fiber films, and apatite had a marked impact on the thermal stability of the collagen fiber film. The improved thermal stability of the composite film was postulated as being the result of apatite facilitating the formation of a compact network structure, which is in agreement with the mechanical and barrier properties. Ghorbani *et al.*[47] also found

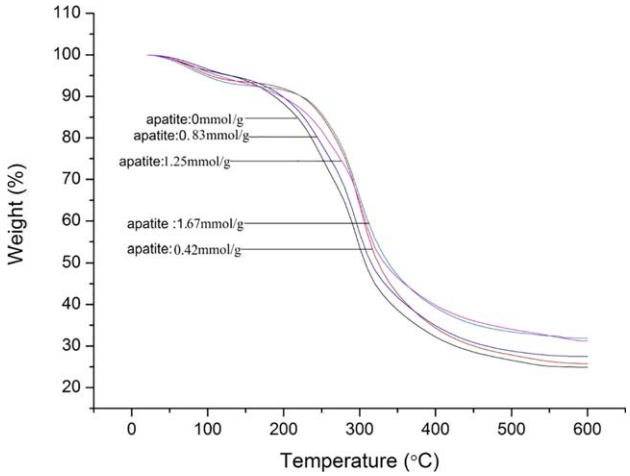

Figure 9. Thermogravimetric curves of films from fish skin gelatin incorporated with apatite at different levels. [Color figure can be viewed in the online issue, which is available at wileyonlinelibrary.com.]

Table II. Thermal Degradation Temperatures and Weight Loss of Collagen Fiber Films Incorporated with Apatite at Different Levels

Apatite content per 1 g collagen (mmol/g)	Δ1		Δ2		Δ3		
	$T_{d1,onset}$ (°C)	Δ_{w1} (%)	$T_{d2,onset}$ (°C)	Δ_{w2} (%)	$T_{d3,onset}$ (°C)	Δ_{w3} (%)	Residue (%)
0	40.92	7.33	202.90	25.91	281.96	43.10	23.66
0.42	45.22	6.98	204.35	23.71	282.00	41.52	27.79
0.83	47.61	6.90	205.87	21.93	281.88	40.00	31.17
1.25	48.21	5.46	211.51	22.06	284.05	41.30	31.18
1.67	55.90	4.16	220.31	17.02	290.66	42.55	36.27

Δ1, Δ2, and Δ3 denote the first-, second-, and third-stage weight losses, respectively, of the films during heating scans.

that hydroxyapatite nanoparticles greatly improved the thermal stability of poly(caprolactone)/chitosan blends.

Differential Scanning Calorimetry

Figure 10 demonstrates the heat endothermic processes of collagen fiber–apatite films, and five endotherms with different peak temperatures could be easily observed. It is noticed that the peak temperatures of the samples climbed from 93.67 °C to 106.93 °C as the content of apatite increased from 0 to 1.67 mmol/g. This might be attributed to the assumption that the presence of apatite accelerates the formation of a densely compact structure, as shown in Figure 7, thus requiring a higher energy for the collagen to degrade.[5] Further, the excellent thermal stability of apatite could also arouse a higher melting temperature.[23,47] And this conclusion corresponds to the thermogravimetric analysis mentioned above.

Scanning Electron Micrographs

Figure 7 depicts the surface and cross section of collagen fiber films with different concentrations (0, 0.42, 1.67 mmol/g) of apatite by SEM. As shown in Figure 7(a–c), *in situ*–produced apatite particles (particle size 1–4 μm) appear as a coating on the surface of the collagen fiber film. Furthermore, the size of the apatite particles gradually increased with the growing amount of disodium hydrogen phosphate and calcium chloride in preparation processing. At the lowest concentration (0.42 mmol/g) of HA, the particle sizes of apatite were mostly below 1 μm; at the highest concentration (1.67 mmol/g) of HA, the apatite particles accumulated and aggregated together and formed larger bundles, which could be easily observed, and the maximum particle size reached 4 μm, as shown in Figure 7(c). This suggested that a collagenous structure of reconstituted collagen fibers could act as nucleator for the formation of apatite crystals.[17] Figure 7(d–f) shows the cross sections of collagen fiber–apatite composite films. Compared to the pure collagen fiber film shown in Figure 7(d), the cross sections of composite films were increasingly even and compact. Owing to the presence of apatite, acting as filler to some extent, the clear, porous net structure of the composite film became less visible. These modifications in the microstructures may facilitate the improvements in the mechanical, barrier, and optical properties and thermostability mentioned in this study.

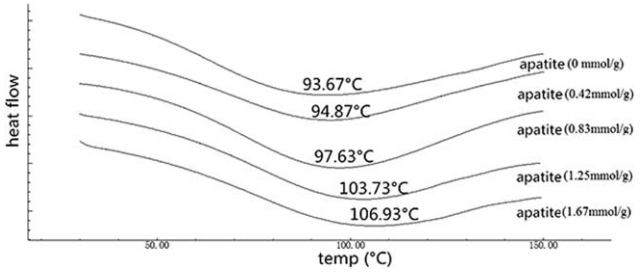

Figure 10. DSC scans of collagen fiber films with different concentrations of apatite.

CONCLUSIONS

In this work, we attempted to use a novel *in situ* synthesis method to prepare apatite and investigated the impact on collagen fiber–apatite composite film performance. The XRD and FTIR results suggested that it is practical to synthesize apatite in collagen fiber films using sodium dihydrogen phosphate and calcium chloride in the presence of ammonia gas at room temperature. The *in situ*–synthesized apatite showed a satisfactory enhancement of the composite film properties. At 1.67 mmol/g apatite, the tensile strength was increased by 30.34% compared to the pure collagen fiber film. The water solubility of collagen fiber–apatite film declined to 10.93% from 14.17% as the apatite concentration ranged from 0 mmol/g to 1.67 mmol/g. The TGA and DSC results suggested that the film with apatite showed higher heat resistance than the pure collagen fiber films. SEM characterized the presence of apatite modifying the poriferous inner structure, and it makes the structure more compact and tougher without obvious disruption. With the enhanced results, it seems that *in situ* synthesis of apatite is a practical reinforcement approach to improving collagen fiber film performance and benefits its potential applications in the food packaging field. But questions on how the apatite and collagen molecules connect, the difference between *in situ* and *ex situ* apatite reinforcement, and whether external ions, such as sodium and ammonia, will influence this enhancement, still need to be answered.

ACKNOWLEDGMENTS

Financial support was kindly supplied by grants from the Special Fund for Agro-scientific Research in the Public Interest of China (No. 201303082) and the National High Technology Research and Development Program of China (No. 2013AA102204).

REFERENCES

1. Bonilla, J.; Vargas, M.; Atarés, L.; Chiralt, A. *Procedia Food Sci.* **2011**, *1*, 50.
2. Galus, S.; Kadzińska, J. *Food Hydrocolloids* **2016**, *52*, 78.
3. Cao, N.; Fu, Y.; He, J. *Food Hydrocolloids* **2007**, *21*, 1153.
4. Sun, Q.; Sun, C.; Xiong, L. *Carbohydr. Polym.* **2013**, *98*, 630.
5. Wang, Y.; Liu, A.; Ye, R.; Wang, W.; Li, X. *Food Chem.* **2015**, *166*, 414.
6. Lee, C. H.; Singla, A.; Lee, Y. *Int. J. Pharm.* **2001**, *221*, 1.
7. Palokangas, H.; Kovanen, V.; Duncan, A.; Robins, S. P. *Matrix* **1992**, *12*, 291.
8. Wang, W.; Zhang, Y.; Ye, R.; Ni, Y. *Int. J. Biol. Macromol.* **2015**, *81*, 920.
9. Friess, W. *Eur. J. Pharm. Biopharm.* **1998**, *45*, 113.
10. Chapman, J. A.; Tzaphlidou, M.; Meek, K. M.; Kadler, K. E. *Electron Microsc. Rev.* **1990**, *3*, 143.
11. Gelse, K. *Drug Deliver. Rev.* **2003**, *55*, 1531.
12. Harper, B.; Barbut, S.; Lim, L.-T.; Marcone, M. *Food Res. Int.* **2012**, *49*, 494.
13. Wolf, K. L.; Sobral, P. J. A.; Telis, V. R. N. *Food Hydrocolloids* **2009**, *23*, 1886.
14. Oechsle, A. M.; Wittmann, X.; Gibis, M.; Kohlus, R.; Weiss, J. *Eur. Polym. J.* **2014**, *58*, 144.
15. Adzaly, N. Z.; Jackson, A.; Villalobos-Carvajal, R.; Kang, I.; Almenar, E. *J. Food Eng.* **2015**, *152*, 24.
16. Karageorgiou, V.; Kaplan, D. *Biomaterials* **2005**, *26*, 5474.
17. Goes, J. C.; Figueiro, S. D.; Oliveira, A. M.; Macedo, A. A.; Silva, C. C.; Ricardo, N. M.; Sombra, A. S. *Acta Biomater.* **2007**, *3*, 773.
18. Sherman, V. R.; Yang, W.; Meyers, M. A. J. *Mech. Behav. Biomed.* **2015**, *52*, 22.
19. Ito, M.; Hidaka, Y.; Nakajima, M.; Yagasaki, H.; Kafrawy, A. H. *J. Biomed. Mater. Res.* **1999**, *45*, 204.
20. Wang, J.; Liu, C. J. *Bionic Eng.* **2014**, *11*, 600.
21. Bhuiyan, D.; Jablonsky, M. J.; Kolesov, I.; Middleton, J.; Wick, T. M.; Tannenbaum, R. *Acta Biomater.* **2015**, *15*, 181.
22. Zhai, Y.; Cui, F. Z. *J. Cryst. Growth* **2006**, *291*, 202.
23. Tampieri, A.; Sandri, M.; Landi, E.; Celotti, G.; Roveri, N.; Mattioli-Belmonte, M.; Virgili, L.; Gabbanelli, F.; Biagini, G. *Acta Biomater.* **2005**, *1*, 343.
24. Chao, S. C.; Wang, M.-J.; Pai, N.-S.; Yen, S.-K. *Mater. Sci. Eng., C* **2015**, *57*, 113.
25. Taguchi, T.; Muraoka, Y.; Matsuyama, H.; Kishida, A.; Akashi, M. *Biomaterials* **2000**, *22*, 53.
26. Tanahashi, M.; Yao, T.; Kokubo, T.; Minoda, M.; Miyamoto, T.; Nakamura, T.; Yamamura, T. *J. Biomed. Mater. Res.* **1995**, *29*, 349.
27. Silva, C.; Thomazini, D.; Pinheiro, A.; Aranha, N.; Figueiro, S.; Goes, J.; Sombra, A. *Mater. Sci. Eng., B* **2001**, *86*, 210.
28. Kato, K.; Eika, Y.; Ikada, Y. *J. Biomed. Mater. Res.* **1996**, *32*, 687.
29. Tanahashi, M.; Matsuda, T. *J. Biomed. Mater. Res.* **1997**, *34*, 305.
30. Miyazaki, T.; Ohtsuki, C.; Akioka, Y.; Tanihara, M.; Nakao, J.; Sakaguchi, Y.; Konagaya, S. *J. Mater. Sci.-Mater. M.* **2003**, *14*, 569.
31. Kawashita, M.; Nakao, M.; Minoda, M.; Kim, H. M.; Beppu, T.; Miyamoto, T.; Kokubo, T.; Nakamura, T. *Biomaterials* **2003**, *24*, 2477.
32. Elżbieta, S.; Maria, S. *Food Chem.* **2007**, *105*, 1302.
33. Kang, N.; Zuo, Y. J.; Hilliou, L.; Ashokkumar, M.; Hemar, Y. *Food Hydrocolloids* **2016**, *52*, 183.
34. Jang, S.; Shin, Y.; Song, K. B. *Int. J. Food Sci. Tech.* **2011**, *46*, 620.
35. Jridi, M.; Souissi, N.; Mbarek, A.; Chadeyron, G.; Kammoun, M.; Nasri, M. *Int. J. Biol. Macromol.* **2013**, *61*, 17.
36. Li, X.; Liu, A.; Ye, R.; Wang, Y.; Wang, W. *Food Hydrocolloids* **2015**, *44*, 390.
37. Rivero, S.; García, M. A.; Pinotti, A. *Innov. Food Sci. Emerg.* **2010**, *11*, 369.
38. Bonilla, J.; Fortunati, E.; Atarés, L.; Chiralt, A.; Kenny, J. M. *Food Hydrocolloids* **2014**, *35*, 463.
39. Tongnuanchan, P.; Benjakul, S.; Prodpran, T. *J. Food Eng.* **2013**, *117*, 350.
40. Fauzi, M. B.; Lokanathan, Y.; Aminuddin, B. S.; Ruszymah, B. H. I.; Chowdhury, S. R. *Mater. Sci. Eng., C* **2016**, *68*, 163.
41. Surewicz, W. K.; Mantsch, H. H. *Biochim. Biophys. Acta, Protein Struct. Mol. Enzymol.* **1988**, *952*, 115.
42. Karimi, F.; Taheri Qazvini, N.; Namivandi-Zangeneh, R. *Int. J. Biol. Macromol.* **2013**, *61*, 102.
43. Farahnaky, A.; Dadfar, S. M. M.; Shahbazi, M. *J. Food Eng.* **2014**, *122*, 78.
44. Żenkiewicz, M.; Richert, J. *Polym. Test.* **2008**, *27*, 835.
45. Mohan, Y. M.; Premkumar, T.; Joseph, D. K. *React. Funct. Polym.* **2007**, *67*, 844.
46. Hoque, M. S.; Benjakul, S.; Prodpran, T. *Food Hydrocolloids* **2011**, *25*, 1085.
47. Ghorbani, F. M.; Kaffashi, B.; Shokrollahi, P.; Akhlaghi, S.; Hedenqvist, M. S. *Mater. Sci. Eng., C* **2016**, *59*, 980.